J Mater Sci: Mater Med (2016) 27:17
DOI 10.1007/s10856-015-5610-4

DELIVERY SYSTEMS

Original Research

Doxorubicin-loaded micelles based on multiarm star-shaped PLGA–PEG block copolymers: influence of arm numbers on drug delivery

Guilei Ma[1] · Chao Zhang[1] · Linhua Zhang[1] · Hongfan Sun[1] · Cunxian Song[1] · Chun Wang[1,2] · Deling Kong[1]

Received: 30 April 2015 / Accepted: 24 October 2015 / Published online: 16 December 2015

Abstract Star-shaped block copolymers based on poly(D,L-lactide-*co*-glycolide) (PLGA) and poly(ethylene glycol) (PEG) (st-PLGA–PEG) were synthesized with structural variation on arm numbers in order to investigate the relationship between the arm numbers of st-PLGA–PEG copolymers and their micelle properties. st-PLGA–PEG copolymers with arm numbers 3, 4 and 6 were synthesized by using different cores such as trimethylolpropane, pentaerythritol and dipentaerythritol, and were characterized by nuclear magnetic resonance and gel permeation chromatography. The critical micelle concentration decreased with increasing arm numbers in st-PLGA–PEG copolymers. The doxorubicin-loaded st-PLGA–PEG micelles were prepared by a modified nanoprecipitation method. Micellar properties such as particle size, drug loading content and in vitro drug release behavior were investigated as a function of the number of arms and compared with each other. The doxorubicin-loaded 4-arm PLGA–PEG micelles were found to have the highest cellular uptake efficiency and cytotoxicity compared with 3-arm PLGA–PEG micelles and 6-arm PLGA–PEG micelles. The results suggest that structural tailoring of arm numbers from st-PLGA–PEG copolymers could provide a new strategy for designing drug carriers of high efficiency.

Graphical Abstract Structural tailoring of arm numbers from star shaped-PLGA–PEG copolymers (3-arm/4-arm/6-arm-PLGA–PEG) could provide a new strategy for designing drug carriers of high efficiency.

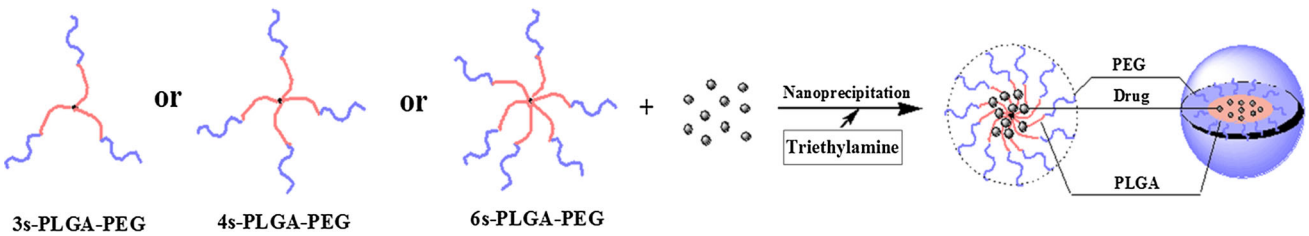

✉ Hongfan Sun
sunhongfan@aliyun.com

✉ Deling Kong
kongdeling@hotmail.com

[1] The Tianjin Key Laboratory of Biomaterials, Institute of Biomedical Engineering, Peking Union Medical College & Chinese Academy of Medical Sciences, Tianjin 300192, China

[2] Department of Biomedical Engineering, University of Minnesota, Minneapolis, MN 55455, USA

1 Introduction

Over the past decades, amphiphilic block copolymers have attracted great interest in their potential application in the biomedical field due to their unique properties of self-assembling into nanoscale micelles in an aqueous environment [1–4]. The unique characteristics, such as core–shell structure, nanoscopic size range and prolonged blood circulation, make the micelles become attractive candidates for drug carrier [5–7]. In general, polymeric micelles can

incorporate hydrophobic pharmaceutical compounds into their hydrophobic cores through physical entrapment, whereas their hydrophilic shell maintains a hydrophilic steric barrier and delays recognition by the reticuloendothelial system (RES) during blood circulation in vivo [8].

Numerous amphiphilic block copolymers have been designed, such as linear copolymers, star-shaped copolymers, grafted copolymers and dendritic copolymers, all sharing the common polymer architecture consisting of both hydrophobic and hydrophilic segments within the same macromolecule [9–12]. The majority of studies on developing amphiphilic block copolymers for micelles preparation have focused on linear block copolymers. Recently, some investigators have paid attention to the synthesis and properties of the star-shaped block copolymers [13–18]. Star-shaped block copolymers contain several linear arms of similar molecular weight that emanate from a central core, representing the simplest examples of branched copolymers. Due to their unique structure, star-shaped block copolymers exhibit different properties from those of their linear counterparts, such as smaller hydrodynamic radius, lower intrinsic viscosity and improvement of micellar stability. Moreover, several recent reports also demonstrated that star-shaped copolymers have some advantages in drug delivery compared to linear copolymers [19–21].

It has been showed that the arm numbers of star-shaped block copolymers have a great influence on the particular characteristics of the micelles, involving morphology, stability, dimensions, and so on [22, 23]. For example, Kim et al. investigated micellar properties of similar block copolymers as a function of the number of arms [23]. In their study, diblock, 3-arm and 4-arm star-shaped amphiphilic copolymers based on poly(ethylene glycol) (PEG) and poly(ε-caprolactone)(PCL) were synthesized. The critical micelle concentration (CMC) decreased in the order of diblock, 3-arm and 4-arm star-shaped amphiphilic copolymers. The size of the micelles increased in the same order as the CMC. The theory of their study also predicted that it is easier to form micelles for 4-arm star-shaped block copolymers than for diblock or 3-arm star-shaped block copolymers.

Even though many studies have been devoted to the formation, dimensions, and morphology of micelles based on amphiphilic star-shaped copolymers with different arm numbers, little attention has been paid to the comparison of feasibility of well-defined star-shaped copolymers with variations on arm numbers as drug carrier. Research on this aspect is very important because polymer structure has substantially influence on various aspects of the drug carrier itself, including drug-loading efficient, drug release behavior and even interaction with cells in vitro [24–26]. However, research in these areas has been neglected.

In the present study, a series of star-shaped copolymers composed of poly(D,L-lactide-*co*-glycolide) (PLGA) as a hydrophobic segment and PEG as a hydrophilic segment were synthesized. Arm numbers 3, 4 and 6 of star-shaped PLGA–PEG copolymers (st-PLGA–PEG) were synthesized by using different cores, such as trimethylolpropane (TMP), pentaerythritol (PTOL) and dipentaerythritol (DPTOL), respectively. The molecular weight and architecture of st-PLGA–PEG with variations on arm numbers were investigated by gel permeation chromatography (GPC) and nuclear magnetic resonance (NMR) spectroscopy. Micellar properties such as CMC, particle size and morphology were analyzed as a function of the number of arms and compared with each other. Subsequently, doxorubicin (DOX), an effective anticancer drug and widely used in cancer therapy, was chosen as a model drug to investigate the influence of st-PLGA–PEG copolymers with different arm numbers on DOX delivery in vitro.

2 Materials and methods

2.1 Materials

Glycolide (GA) (mp 83.5–84.5 °C, 99 %) and D,L-lactide (DLLA) (mp 126.5–127.5 °C, 99 %) were purchased from Beijing Yuanshengrong Technology Co. Ltd. (China). TMP (99 %), PTOL (99 %) and DPTOL (99 %) were obtained from Tianjin Fuchen Chemical Company (China). Poly (ethylene glycol)-bis-amine (PEG-bis-amine) (Mw = 4000 g/mol) was purchased from Beijing Kaizheng Technology Co., LTD. (China). Stannous octoate ($Sn(Oct)_2$), 1-ethyl-3-(3-dimethylaminopropyl)-carbodi-imide hydrochloride (EDC, 99 %), *N*-hydroxy succinimide (NHS, 99 %), triethylamine (TEA), dicyclohexyl carbodiimde (DCC, 99 %) and PLGA (75:25, Mw = 66,000–107,000 g/mol) were obtained from Sigma-Aldrich Corporation. Doxorubicin (DOX, 99 %) was supplied by Dalian Meilun Pharmaceutical Co. Ltd. (China). Cell Counting Kit-8 (CCK-8) was purchased from Dojindo Molecular Technologies Inc. (Japan). All other chemicals used were of the highest quality commercially available.

2.2 Characterization of copolymers

A VARIAN UNITY-plus 400-MHz proton NMR spectrometer (Varian, USA) was used for ^{1}H NMR and ^{13}C NMR in $CDCl_3$ to study the molecular structure and composition of the synthesized copolymers. Molecular weight and molecular weight distribution of copolymers were determined using Waters and comprised following equipment: a Waters 515 HPLC pump, a Waters styragel Columns (Styragel HR 0.5–2 and 4), and a Waters 410 Differential Refractometer. The effective molecular weight ranges are 0–1000, 500–20,000 and 5000–600,000 g/mol, respectively. Tetrahydrofuran was used as an eluting

solvent at a flow rate of 1.0 mL/min at 35 °C, and polystyrene standards were used as the calibration sample.

2.3 Synthesis of star-shaped PLGA–PEG copolymers (st-PLGA–PEG)

All the st-PLGA–PEG copolymers were synthesized by ring-opening polymerization. Variation in the number of arms was accomplished by using different initiator, such as TMP (3 arms), PTOL (4 arms) and DPTOL (6 arms), respectively. On the basis of different arm numbers (*n*), the resulting st-PLGA–PEG of this study were named as *n*s-PLGA–PEG, where $n = 3$, 4 or 6 arms. 3s-PLGA–PEG, 4s-PLGA–PEG and 6s-PLGA–PEG copolymers were prepared via a three-step synthetic strategy: First, st-PLGA with different arms were successfully synthesized via the ring-opening polymerization of DLLA and GA using commercial primary alcohols such as TMP, PTOL or DPTOL as initiators in the presence of catalytic amount of $Sn(Oct)_2$; Second, st-PLGA–COOH was synthesized by the carboxylation of st-PLGA with succinic anhydride; Finally, the 3s-PLGA–PEG, 4s-PLGA–PEG or 6s-PLGA–PEG copolymers were obtained by conjugation of st-PLGA–COOH and PEG-dis-amine. Typically, the 4s-PLGA–PEG copolymer was synthesized through three steps, which are detailed as following (Fig. 1).

2.3.1 Synthesis of 4-arm star-shaped PLGA (4s-PLGA)

DLLA (10.0 g, 69.4 mmol), GA (2.68 g, 23.1 mmol), PTOL (0.088 g, 0.62 mmol) and $Sn(Oct)_2$ (3.78 mg, 9.3 μmol) were added into a silanized glass tube, which was connected to a vacuum system. An exhausting-refilling process with high purity nitrogen was repeated three times and the mixture kept vacuum (20–30 Pa) about 30 min. The tube was sealed and reacted at 160 °C for 10 h. The resulting product was dissolved in methylene chloride and then poured into excess methanol to precipitate the polymerized product. The purified copolymer was dried in a vacuum oven at 40 °C for 48 h.

^{13}C NMR (100 MHz, $CDCl_3$, δ, ppm): 169.490, 169.478 and 168.905(C=O of DLLA), 166.622, 166.617 and 166.103(C=O of GA), 69.604, 69.209 and 69.205 (CH of DLLA), 67.319, 66.908 and 66.907 (C of PTOL), 61.457, 60.999 and 60.997 (CH_2 of GA), 21.494, 20.650 and 20.463 (CH_2 of PTOL), 17.760, 16.863 and 16.862 (CH_3 of DLLA). ^1H NMR (400 MHz, $CDCl_3$, δ, ppm): 5.20 (m, 1H, CH of DLLA), 4.82 (m, 2H, CH_2 of GA), 1.56 (d, 3H, CH_3 of DLLA, J = 6.3 Hz).

2.3.2 Synthesis of 4-arm star-shaped PLGA–PEG copolymers (4s-PLGA–PEG)

The 4s-PLGA–PEG copolymers were then synthesized using condensation reaction between the carboxyl group of 4s-PLGA–COOH and the amide group of PEG-bis-amine at room temperature [27]. First, 4s-PLGA was carboxylated with succinic anhydride to produce 4s-PLGA–COOH. Second, 4s-PLGA–COOH (0.2 mmol, 3.6 g) was dissolved in 25 mL of methylene chloride. DCC (247.6 mg, 1.2 mmol), NHS (138.6 mg, 1.2 mmol) and DMAP (146.6 mg, 1.2 mmol) were added into the polymer solution under magnetic stirring. Activation of the carboxylic acid end group in 4s-PLGA–COOH was accomplished for 24 h at room temperature. Insoluble dicyclohexylurea was removed by filtration, and the polymer with an activated carboxylic group was isolated by precipitation into anhydrous diethyl ether. The polymer precipitant was dried under vacuum. Finally, the coupling reaction of PEG-bis-amine to the activated 4s-PLGA–COOH was carried out by adding an excess amount of PEG-bis-amine. Activated 4s-PLGA–COOH (1.8 g, 0.1 mmol) and PEG-bis-amine (4 g, 1 mmol) were reacted in 50 mL of chloroform for 48 h at room temperature with stirring. The resulting product was precipitated by slowly dropping into cold methanol. The collected product was washed with an excess amount of cold methanol and dried under vacuum.

^1H NMR (400 MHz, $CDCl_3$, δ, ppm): 5.20 (m, 1H, CH of DLLA), 4.82 (m, 2H, CH_2 of GA), 3.65 (s, 4H, CH_2 CH_2O of PEG), 1.56 (d, 3H, CH_3 of DLLA, J = 5.7 Hz)

$$\mathrm{Mn,\ GPC} = 33{,}186\,\mathrm{g/mol}, \mathrm{Mw, GPC} = 39{,}133\,\mathrm{g/mol},\ \mathrm{Mw/Mn} = 1.18.$$

2.4 Preparation of DOX-Loaded St-PLGA–PEG Micelles

DOX-loaded st-PLGA–PEG micelles were prepared by a modified nanoprecipitation method using an acetone–water system. Briefly, 100 mg of st-PLGA–PEG copolymers, 11.1 mg of DOX were dissolved in 5 mL of acetone in the presence of 3.8 mg of TEA. This mixture was dropwise added into 25 mL water under magnetic stirring at 150 rpm. The resulting suspension was then stirred overnight at room temperature to remove acetone completely. The micelles suspension was centrifuged at 25,000 rpm for 30 min and then washed three times to remove unencapsulated drug. Finally, the dispersed solution was lyophilized for two days. Blank st-PLGA–PEG micelles were prepared in a similar manner without adding DOX.

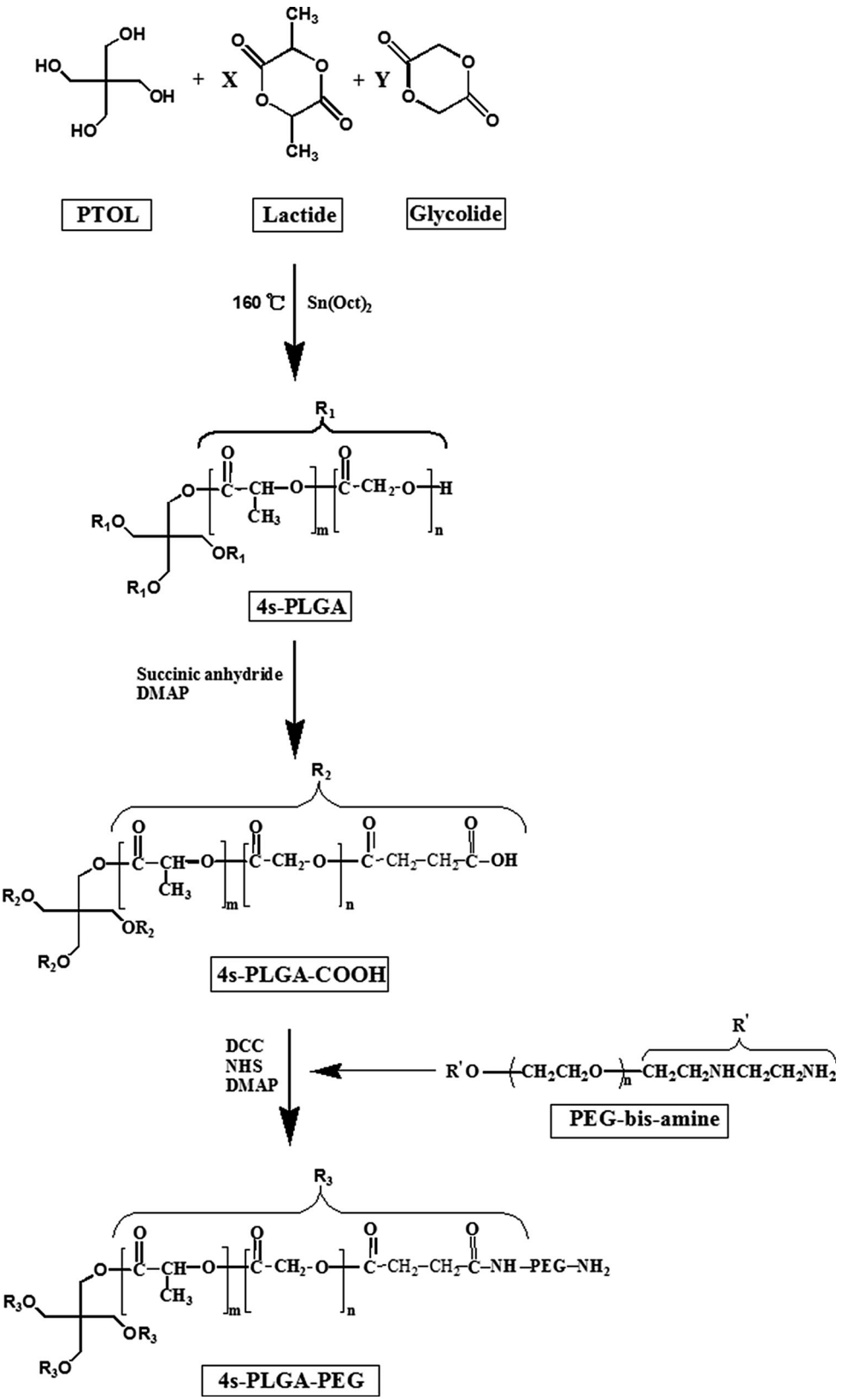

Fig. 1 Example synthesis of amphiphilic star-block copolymers based on PLGA and PEG with PTOL as the initiator

2.5 Critical micelle concentration determination

The CMC of st-PLGA–PEG block copolymers in water was determined with a fluorescence spectrophotometer (F-4500, Hitachi, and Tokyo, Japan). Pyrene was used as the fluorescence probe. The fluorescence excitation spectra of pyrene were measured at various concentrations of st-PLGA–PEG micelles as previously described [28, 29]. In brief, 100 mg of st-PLGA–PEG copolymers was dissolved in 5 mL of acetone. The resulting solution was dropwise added into 50 mL of water under magnetic stirring to yield micelles. After the acetone was removed by evaporation, the micelles solution was diluted with water to various concentrations. The concentration of micelles ranged from 5.0×10^{-5} to 1.0 mg/mL and the pyrene concentration was fixed at 6.0×10^{-7} mol/L. The fluorescence excitation spectra were measured at emission wavelength of 390 nm. The slit width for both excitation and emission was 1.5 nm. The ratio of fluorescence intensity at 334 and 337 nm (I_{337}/I_{334}) was calculated and plotted against the logarithm of the copolymer concentrations.

2.6 Characterization of DOX-loaded micelles

The mean size and size distribution of the prepared micelles were determined by dynamic light scattering (DLS) using NY 90-Plus particle size analyzer (Brookhaven Instruments Corporation, Holtsville, NY). Before measurement, the freshly prepared particles were appropriately diluted. Zeta potential of the prepared micelles was also measured using a zeta potential analyzer (ZetaPALS; Brookhaven Instruments Corporation, Holtsville, NY). The data were obtained with the average of three measurements.

The morphology of the st-PLGA–PEG micelles was examined by transmission electron microscope (TEM) (Tecnai-F20, FEI, The Netherlands). To prepare specimens for TEM, a drop of micelle solution was deposited onto a carbon-coated copper grid and was allowed to air-dry.

The amount of DOX in the lyophilized micelles was determined by fluorescence spectrometer (excitation at 485 nm and emission at 590 nm). 2 mg of lyophilized micelles were dissolved in 5 mL of dimethyl sulphoxide (DMSO). Calibration curve was obtained with DOX/DMSO solutions with different DOX concentrations. Drug encapsulation efficiency was defined as the ratio of DOX detected in micelles to that of the total drug used for micelles preparation.

2.7 In vitro drug release studies

In vitro release study of DOX from DOX-micelles was determined in phosphate-buffered solution (PBS) at 37 °C. Briefly, 5 mg of micelles were dispersed in 5 mL of above buffer to form a suspension and subsequently put into dialysis tube with a molecular weight cutoff of 1000 Daltons. The dialysis tube was then immersed in 20 mL of release medium and stirred at a speed of 120 rpm at 37 °C. A whole-medium change method was used for prevention of drug saturation in the drug release study. At appropriate intervals, the whole medium was withdrawn and replaced with an equal volume of fresh PBS. The amount of released DOX in the PBS was determined by fluorescence spectrometer as mentioned above. Data were expressed as mean value of three independent experiments with the reported standard deviation.

2.8 Cellular uptake studies

Human cervix carcinoma cells (HeLa) were obtained from the Institute of Biochemistry and Cell Biology, Chinese Academy of Sciences (Shanghai, China). Cells were incubated in RPMI 1640 medium with 10 % heat-inactivated fetal bovine serum, 100 IU/mL penicillin and 100 μg/mL streptomycin. The culture was maintained in 95 % air humidified atmosphere containing 5 % CO_2 at 37 °C.

2.8.1 Quantitative studies through flow cytometry

DOX is colored and has a fairly strong self-fluorescence in the visible region. Thus, no additional fluorescence marker was needed for this experiment. For flow cytometry studies, the cells were seeded in six-well culture plates (1×10^5 cells per well) and incubated in RPMI 1640 medium (2 mL per well) for 24 h. The cells were then incubated with free DOX (5 μg/mL) or DOX-micelles (equivalent DOX concentration: 5 μg/mL) for 4 h. Then, cells were rinsed three times with PBS and harvested using Trypsin-Ethylenediaminetetraacetic acid (EDTA) and fixed by 1 % paraformaldehyde. Cell density was adjusted to 1×10^6 cells/mL and 1 mL of this cell suspension was used to measure the cellular uptake of DOX by an FACSCalibur flow cytometer (BD Biosciences).

2.8.2 Qualitative analysis by confocal laser scanning microscopy

For confocal laser scanning microscope studies, the cells were seeded onto 35 mm glass bottom culture dish (1×10^5 cells per dish) and incubated in RPMI 1640 medium (1 mL per dish) for 24 h. Cells were treated with free DOX (5 μg/mL) or DOX-micelles (equivalent DOX concentration: 5 μg/mL) for 4 h. Then, cells were rinsed three times with PBS and fixed with ethanol. Cells were stained with 50 nM LysoTracker Green (Molecular Probe,

Invitrogen, USA) for 30 min and washed twice with PBS. Finally, cells were observed by confocal laser scanning microscope (CLSM 410; Zeiss, Jena, Germany) with imaging software Fluoview FV500.

2.9 Cytotoxicity evaluation

CCK-8 assay was used for cell viability of DOX-loaded st-PLGA–PEG micelles [30]. Briefly, HeLa cells were seeded onto 96-well culture (1×10^4/well) using RPMI 1640 medium for 24 h. Then the cells were incubated with empty st-PLGA–PEG micelles (polymer concentration of 0.25, 0.5, 1, 1.5 and 2 mg/mL), free DOX and DOX-loaded st-PLGA–PEG micelles (equivalent DOX concentration of 1.56, 3.12, 6.25, 12.5 and 25 μg/mL, and the st-PLGA–PEG polymer in the DOX-loaded micelles with concentration ranging from 21 to 330 μg/mL), respectively. At designed time intervals, the medium was removed and the wells were washed three times with PBS. Ten microliters of CCK-8 solution was added to each well of the plate and incubated for a further 4 h. The absorbance at 450 nm was measured using a thermo varioskan flash multifunction microplate reader.

2.10 Statistical analysis

Data were expressed as mean ± standard deviation (SD). Statistical significance of differences was assessed by Student's *t* test or ANOVA followed by the Tukey's multiple comparison. A probability value of <0.05 was considered significant, and $P < 0.01$ was considered very significant.

3 Results and discussion

3.1 Synthesis and characterization of st-PLGA–PEG block copolymers with different arms

The goal of this work was to evaluate the potential of micelles formed by amphiphilic st-PLGA–PEG copolymers with the same arm length but different arm numbers in drug delivery applications. Well-defined st-PLGA–PEG block copolymers with different arms, such as 3s-PLGA–PEG, 4s-PLGA–PEG and 6s-PLGA–PEG, were prepared via a three-step synthetic strategy as described above.

The chemical structure of PLGA, 3s-PLGA, 4s-PLGA and 6s-PLGA was investigated via ^{13}C NMR spectrum (Fig. 2). In the ^{13}C NMR spectrum of PLGA, the signals were observed at *a* (δ = 17 ppm, CH_3 of DLLA units in PLGA segments), *b* (δ = 69 ppm, CH of DLLA units in PLGA segments), *c* (δ = 61 ppm, CH_2 of GA units in PLGA segments), *d* (δ = 168 ppm, C=O of DLLA units in PLGA segments) and *e* (δ = 166 ppm, C=O of GA units in PLGA segments), respectively. In comparison with the ^{13}C NMR spectrum of PLGA, new signals appeared indicated successful synthesis of 3s-PLGA, 4s-PLGA or 6s-PLGA. Namely, signals at 67 ppm are assigned to the methylene carbon of TMP, PTOL or DPTOL units and signals at 21 ppm are in correspondence with the quaternary carbon of the of TMP, PTOL or DPTOL units. The chemical structure of st-PLGA–PEG copolymers were confirmed by ^1H spectroscopy. The successful synthesis of st-PLGA–PEG was determined mainly by the appearance

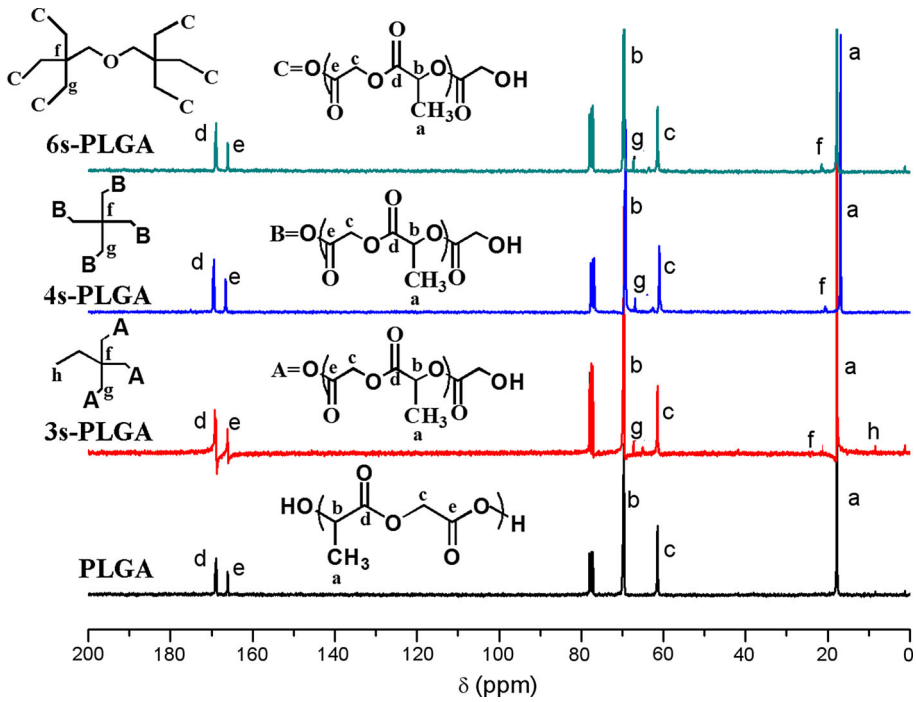

Fig. 2 The ^{13}C NMR spectra of PLGA, 3s-PLGA, 4s-PLGA and 6s-PLGA

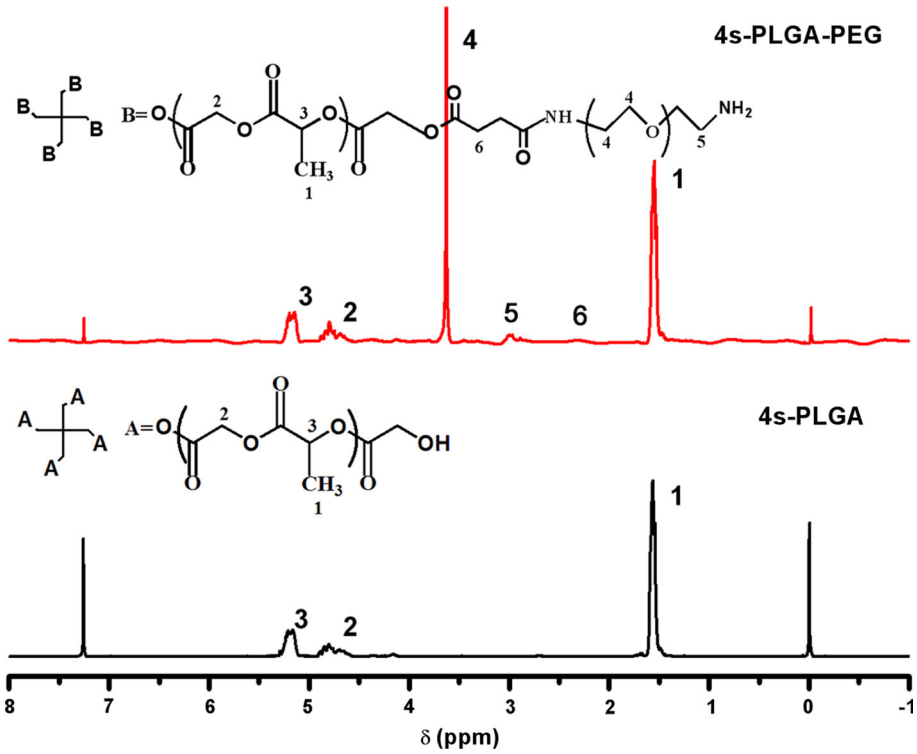

Fig. 3 The ^{1}H NMR spectra of 4s-PLGA and 4s-PLGA–PEG copolymers

Table 1 Molecular characteristics of st-PLGA–PEG block copolymers with different arms

Sample	Mn (g/mol)[a] PLGA in each arm	LA:GA[a]	Mw (g/mol)[b] copolymer	Mn (g/mol)[b]	Mw/Mn[b]	Yield (wt%)
3s-PLGA	–	3.03	15,600	11,734	1.32	77.25
4s-PLGA	–	3.01	23,190	18,266	1.26	76.74
6s-PLGA	–	3.01	27,736	23,208	1.19	78.07
3s-PLGA–PEG	4201	3.03	28,674	23,644	1.20	75.34
4s-PLGA–PEG	4569	3.01	39,133	33,186	1.18	76.28
6s-PLGA–PEG	4314	3.01	60,257	46,328	1.29	77.13

[a] Detemined by ^{1}H NMR spectra: molecular weight of PLGA block was determined by using the integration ratio of resonance due to PEG blocks at 3.6 ppm and PLGA blocks at 4.76 ppm in ^{1}H NMR spectra

[b] Measured by GPC

of the peaks of $\delta = 1.6$ ppm (CH_3 of DLLA units in PLGA segments), $\delta = 4.8$ ppm (CH_2 of GA units in PLGA segments), and $\delta = 5.2$ ppm (CH of DLLA units in PLGA segments). The high intensity of the peak at $\delta = 3.6$ ppm indicates the existence of the PEG main chain (Fig. 3).

The molecular weights, polydispersity and composition of st-PLGA–PEG copolymers with different arm numbers determined by ^{1}H NMR and GPC are summarized in Table 1. The number-average molecular weights *Mn* obtained from GPC were somewhat lower than those *Mn* determined from ^{1}H NMR. This is generally attributed to the inevitable decrease in the hydrodynamic volume imposed by branching, which in turn exceeds the relative discrepancy with the polystyrene standards [31, 32]. The 3-arm, 4-arm or 6-arm st-PGA-PEG copolymers had narrow polydispersity index (PDI) varying from 1.18 to 1.29. Unimodal GPC trace with low polydispersity value confirmed the successful formation of star-shaped block copolymers (Fig. 4).

3.2 Critical micelle concentration (CMC)

As summarized in Fig. 5, the CMC values of st-PLGA–PEG copolymers depended upon the number of arms in the star-shaped copolymers, which was in the range of 1.78×10^{-3}–6.30×10^{-3} mg/mL. The CMC decreased in the order of 3-arm, 4-arm and 6-arm star-shaped PLGA–PEG copolymers, which is similar to the results reported by Kim et al. [23]. Kim et al. reported that the CMC decreased with increase the arm number of star-shaped PEG–PCL

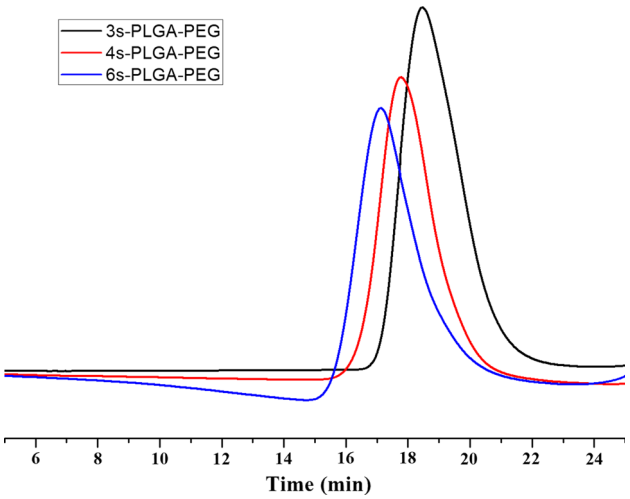

Fig. 4 GPC traces of st-PLGA–PEG copolymers with different arm numbers

copolymer. This is probably because the covalent bond character of star-shaped block copolymers facilitates micellization since the unimer state of star-shaped block copolymers with many arms resembled the micellar state, and indicating that the micelles were easily formed when the number of arms in copolymers increased.

3.3 Preparation and characterization of DOX-loaded micelles

DOX-loaded st-PLGA–PEG micelles were prepared by a nanoprecipitation method with acetone as a suitable solvent. Figure 6a schematically describes the preparation of DOX-loaded st-PLGA–PEG micelles. As shown in Fig. 6a, the hydrophilic segment PEG of st-PLGA–PEG copolymers is expected to be oriented outside, while the hydrophobic segment PLGA of st-PLGA–PEG copolymers is buried in the core entrapping DOX. To increase the loading amount of DOX in the internal core of micelles, an excess amount of TEA was added into the acetone solution. TEA played an important role in transforming water-soluble DOX into a water-insoluble form by scavenging chloride ion of DOX salt form. Several studies previously reported an increase in DOX loading within nanoparticulate drug carriers when free DOX was encapsulated in the presence TEA [33].

3.3.1 Size, zeta potential, morphology and drug encapsulation efficiency

Particle size is an important property of micelles in the consideration of their performance in vivo [34]. The mean hydrodynamic size from DLS studies of the DOX-loaded micelles was 85.1 ± 3.5 nm for 3s-PLGA–PEG, 122.4 ± 4.7 nm for 4s-PLGA–PEG and 208.8 ± 5.2 nm for 6s-PLGA–PEG, which is in the appropriated size range for reducing uptake by the RES and prolonging the circulation time in the blood (Fig. 6b; Table 2) [35]. This increase in micelles size with an increase in arm numbers of st-PLGA–PEG copolymers is in accordance with the results reported by other researchers [23]. The particle sizes of blank micelles prepared from st-PLGA–PEG copolymers with different arm numbers were also studied. The DOX-loading caused an

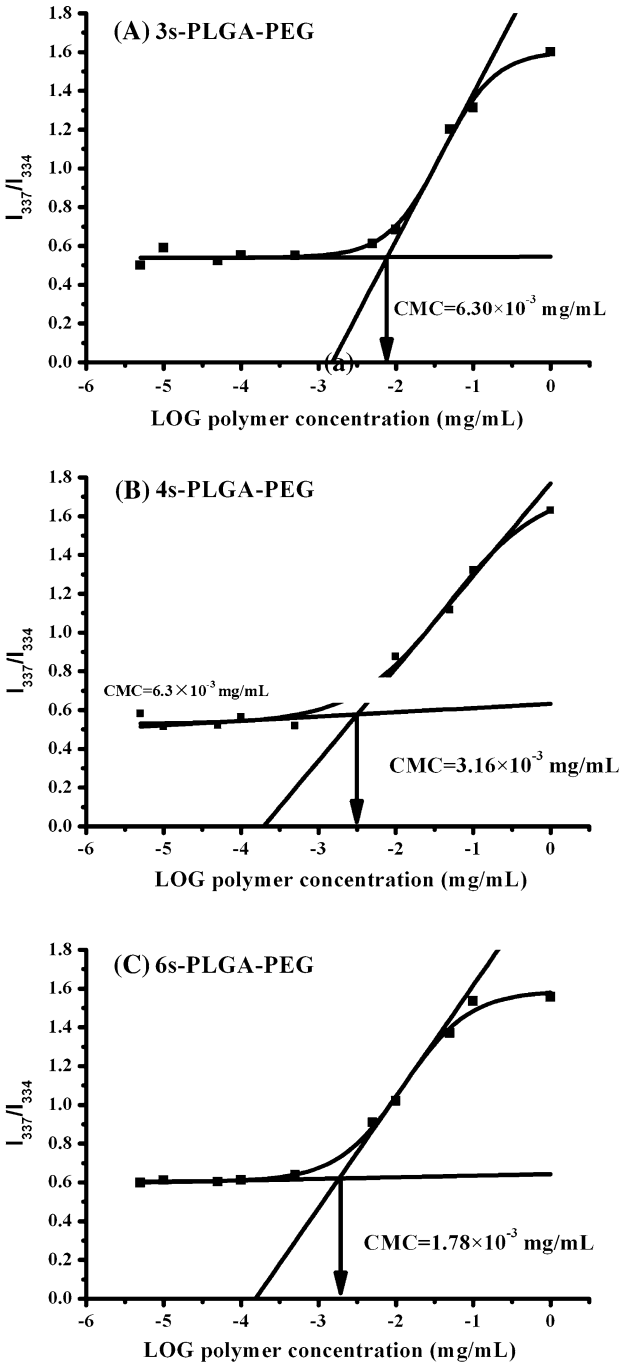

Fig. 5 Plots of the intensity ratio (I_{337}/I_{334}) against the concentration of **a** 3s-PLGA–PEG, **b** 4s-PLGA–PEG, and **c** 6s-PLGA–PEG

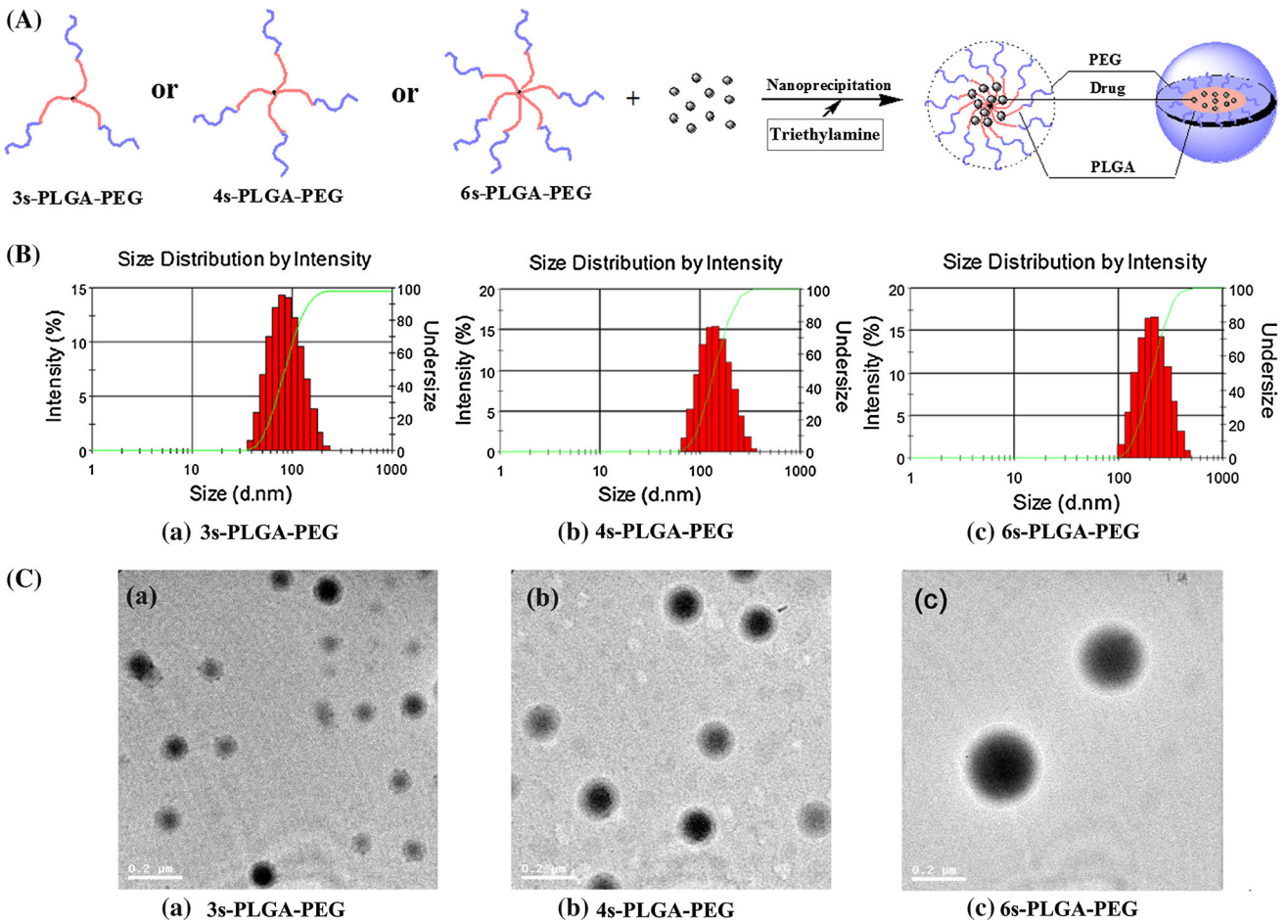

Fig. 6 **a** Schematic illustration of DOX-loaded micelles based on st-PLGA–PEG copolymers. **b** Size distribution of *a* 3s-PLGA–PEG micelles, *b* 4s-PLGA–PEG micelles, and *c* 6s-PLGA–PEG micelles. **c** TEM images of *a* 3s-PLGA–PEG micelles, *b* 4s-PLGA–PEG micelles, and *c* 6s-PLGA–PEG micelles

Table 2 Characterization of DOX-loaded st-PLGA–PEG micelles

Copolymer	Size (nm)	PDI	Zeta potential (mv)	Drug loading (%, w/w)	Encapsulation efficiency (%)
3s-PLGA–PEG	85.1 ± 3.5	0.17	−18.6 ± 2.1	6.98 ± 0.2	70.1 ± 2.9
4s-PLGA–PEG	122.4 ± 4.7	0.13	−15.7 ± 2.5	7.49 ± 0.3	75.2 ± 3.2
6s-PLGA–PEG	208.8 ± 5.2	0.15	−13.4 ± 3.2	7.82 ± 0.2	78.5 ± 3.6

PDI polydispersity index, n = 3

increase of approximately 20 nm in size compared with blank micelles. The reason might be that the encapsulation of hydrophobic DOX could promote hydrophobic interaction among the PLGA chains and consequently increase the micelle aggregation, which leads to larger size [36, 37]. In addition, there was no obvious change in the narrow size distributions of micelles with DOX loading.

Zeta potential is an important factor for the stability of the micelles in suspension. The mutual repulsion of charged micelles can maintain the good physical stability profile of micelle dispersion. As shown in Table 2, zeta potential was negative for all micelles and decreased in the order of 3-arm, 4-arm and 6-arm star-shaped copolymers. A different PEG distribution onto micelle surface as a consequence of the different arm numbers of st-PLGA–PEG copolymers can be responsible of this effect [38]. The slightly negative charge of DOX-loaded st-PLGA–PEG micelles may reduce the undesirable clearance by RES such as liver, improve the blood compatibility, thus deliver micelles more efficiently to the tumor sites [39].

A typical TEM image of micelles was visualized in Fig. 6c. The TEM picture clearly shows a well-defined core–shell structure of the corresponding micelles. In general the trend in diameters of st-PLGA–PEG copolymer with different arm numbers, as observed by TEM, was in good agreement with that observed by DLS. However, the diameters by TEM were found to be a smaller than the values determined by DLS studies. This difference in micelles size measured by TEM and DLS should be attributed to that the latter is the hydrodynamic diameter of micelles in water, whereas the former reveals the morphology size of the micelles in dry state [40].

The effects of the arm numbers of st-PLGA–PEG copolymers on the drug loading content and encapsulation efficiency were investigated. As shown in Table 2, all the st-PLGA–PEG copolymers exhibited efficient drug encapsulation. The drug loading content and encapsulation efficiency of DOX in the st-PLGA–PEG micelles had an increased tendency over the arm numbers of st-PLGA–PEG copolymers, and it was in the order of 3s-PLGA–PEG < 4s-PLGA–PEG < 6s-PLGA–PEG. There are a number of possible explanations for the increased efficiency, including those st-PLGA–PEG copolymers with increasing arm numbers form larger micelles with more payload capacity or that the stronger binding affinity between hydrophobic DOX and the core region PLGA more strongly favors drug encapsulation for the st-PLGA–PEG copolymers with many arms.

3.3.2 In vitro drug release

The in vitro release behavior of DOX from st-PLGA–PEG micelles with different arm numbers was studied under a simulated physiological condition (PBS, pH 7.4) and an acidic condition (PBS, pH 5.8) at 37 °C. These pH values were selected to represent extracellular pH values (pH 7.4) and endosomal or lysosomal pH values (pH 5–6). As shown in Fig. 7, the release profile was characterized by a rapid release at the early stage (up to 5 day) followed by a more slower release stage (up to 21 day) regardless of pH. The sustained release likely resulted from continued diffusion of DOX through the hydrophobic PLGA inner of the micelles [41]. During this stage DOX cumulative release decreased with increasing numbers of arms in the st-PLGA–PEG copolymers, which is probably that st-PLGA–PEG copolymer with many arms forms more compact core [20]. Furthermore, the effect of drug loading amount on the drug release rate from micelles should also be taken into account. It was shown previously that higher drug loading resulted in slower drug release [42].

Generally the release of DOX from the drug carriers was pH dependent probably due to the increase in solubility of DOX at lower pH [43, 44]. As a result, DOX cumulative release would be expected to increase with decreasing pH of the release medium. Figure 7 clearly showed that the release of DOX from st-PLGA–PEG micelles in the acidic environment (pH5.8) was much faster than that in physiological environment (pH7.4). This pH-sensitive releasing behavior is useful for tumor-targeted DOX delivery with micelles. An accelerated release will occur once the micelle particles were internalized into the endosome or lysosome of solid tumor site where the pH value is much lower.

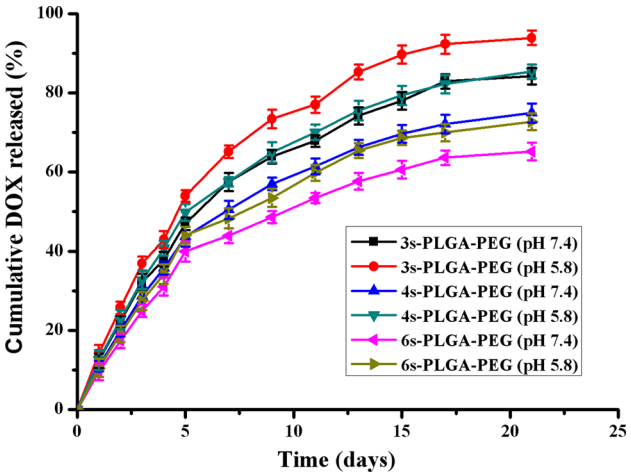

Fig. 7 The in vitro release profile of DOX-loaded micelles based on st-PLGA–PEG copolymers (n = 3)

3.4 Cellular uptake of DOX-loaded st-PLGA–PEG micelles

Cellular uptake of DOX-loaded st-PLGA–PEG micelles was evaluated in HeLa cells by flow cytometry and CLSM. Since DOX itself is fluorescent, it was used directly to visualize and analyze cellular uptake of the micelles. Figure 8 presents the flow cytometric measurements of accumulation of DOX-loaded st-PLGA–PEG micelles in HeLa cells. It can be seen from Fig. 8 that the free DOX demonstrated much lower cellular uptake than DOX-loaded micelles, which may be attributed to the multi-drug resistance (MDR) effect for the free drug since DOX has been found to be a substrate of P-glycoprotein which are rich in the cancer cells [45, 46].

Intracellular uptake was different for st-PLGA–PEG micelles with different arm numbers. 4s-PLGA–PEG micelles resulted in about threefold higher cellular uptake than that of 3s-PLGA–PEG micelles and 6s-PLGA–PEG micelles. The difference in particle size among st-PLGA–PEG micelles could partially explain the observed differences in their cellular uptake. A number of systematic studies evaluating particle size-dependent cellular uptake have been reported in the literature; [47, 48] they found

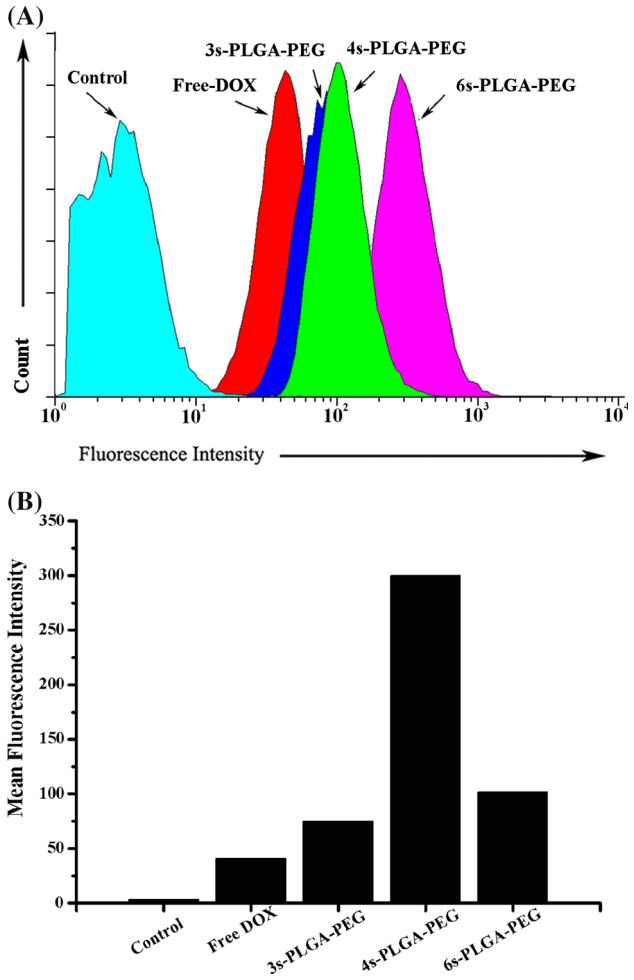

Fig. 8 **a** Flow cytometry analysis of DOX fluorescence intensity of HeLa cells incubated with DOX-loaded st-PLGA–PEG micelles at 37 °C for 4 h. **b** DOX mean fluorescence intensity of the HeLa cells incubated with DOX-loaded st-PLGA–PEG micelles with different arm numbers at 37 °C for 4 h. Untreated cells were used as control

that particle size can affect the efficiency and pathway of cellular uptake by influencing the adhesion of the particles and their interaction with cells. Generally, there existed a critical size below which the uptake rate increased with increasing particle size and up which the uptake rate decreased with increasing size. In this paper, the prepared the DOX-loaded 4s-PLGA–PEG micelles with the particle size of about 120 nm showed the maximum cellular uptake. It was concluded that the cell uptake of st-PLGA–PEG micelles was size-dependent in HeLa cells.

Furthermore, the architecture of multiarm st-PLGA–PEG copolymer with different arm numbers forming the micelles may have also contributed to the observed differences in cellular uptake of st-PLGA–PEG micelles [21, 49]. It is possible that the covalent bond character of star-shaped block copolymers and PEG chain flexibility at the PLGA/PEG junction points results in the formation of PEG domains distributed differently on the surface of st-PLGA–PEG micelles. This hypothesis is in agreement with the findings of Fabiana et al. who demonstrated that micelles obtained from amphiphilic poly(ε-caprolactone)(PCL)-PEG triblock and star-shaped diblock copolymers have a different cellular uptake [21]. It was highlighted that the PEG distribution on the micelles surface is an important feature which governs the extent of micelle transport inside cells. Nevertheless, further studies on PEG distribution on surface of st-PLGA–PEG micelles with different arm numbers are needed to provide more detailed information about micelle–cells interactions.

To investigate the intracellular distribution of DOX-loaded micelles in the HeLa cells, CLSM was performed (Fig. 9). After 4 h of incubation with free DOX, DOX fluorescence was observed in both the nucleus and the cytoplasm, consistent with the results of previous studies (Fig. 9a) [50]. In the case of the three micelle formulations (Fig. 9b–d), DOX fluorescence was observed mainly in cytoplasm instead of nucleus, which was due to the different cellular uptake mechanisms of free DOX and micelles. The free DOX could pass through the cell membrane by diffusion which is driven by a concentration gradient across the membrane, while micelles were taken up by endocytosis which is both time- and energy-consuming [51, 52].According to the CLSM results, intracellular free DOX molecules in the cytosol were rapidly transported to the nucleus and avidly bound to the chromosomal DNA. However, the DOX micelles were initially located within the endosomal or lysosomal intracellular compartements, releasing DOX in a sustained manner, and then diffused into the cytosol before it finally entered the cell nuclei.

3.5 In vitro cytotoxicity

Cytotoxic effects of free DOX, DOX-loaded st-PLGA–PEG micelles and empty st-PLGA–PEG micelles were studied using the cck-8 assay against cultured HeLa cells as shown in Fig. 10. Empty st-PLGA–PEG micelles did not exhibit obvious cytotoxicity to cells during the test period,proving the commendable biocompatibility of micelles with concentration ranging from 0.25 to 2 mg/mL. As expected, the cytotoxicity of DOX increased with increasing dose and time. Compared with DOX-loaded micelles, free DOX showed higher cytotoxicity against tumor cells employed during the test period. As previously discussed, the fast diffusion of free DOX into the cell nuclei (as shown in Fig. 9a) might be the reason for this observation. Like all anthracyclines, DOX is a DNA intercalator, which inhibits DNA replication in rapidly growing cancer cells [53]. In contrast, DOX-

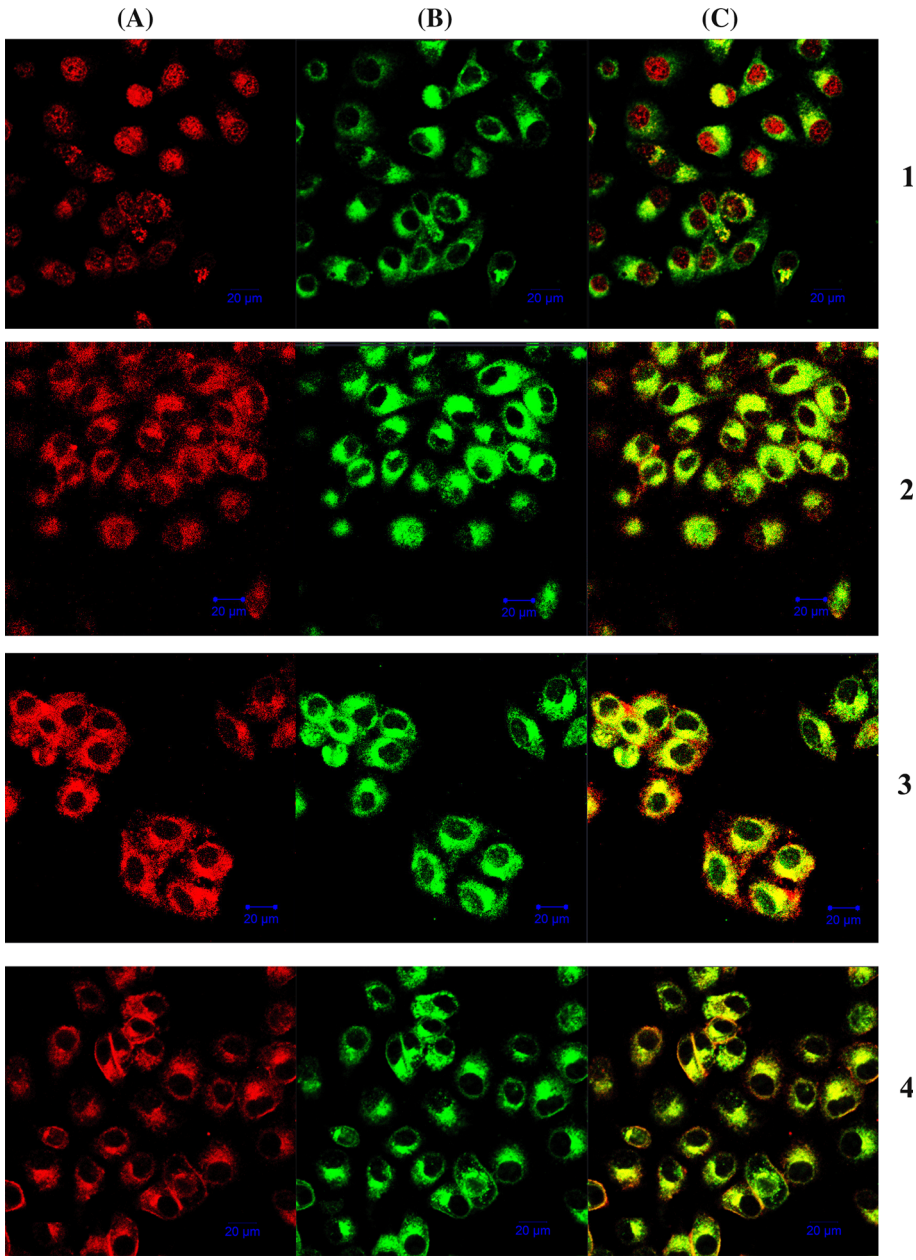

Fig. 9 CLSM images of HeLa cells after 4-h incubation with **a** free DOX, **b** DOX-loaded 3s-PLGA–PEG micelles, **c** DOX-loaded 4s-PLGA–PEG micelles, and **d** DOX-loaded 6s-PLGA–PEG micelles. For each *panel*, images from *left* to *right* show DOX fluorescene in cells (*red*), lysosome stained by LysoTracker (*green*), and overlays of two images (*yellow*) (Color figure online)

loaded micelles have to be internalized by endocytosis, release the loaded drugs into the cytosol region (as shown in Fig. 9b–d) in a sustained manner, and then diffuse into the nuclear regions. Thus, this requires adequate time for doxorubicin DOX-loaded micelles to show cytotoxicity.

The IC_{50} values of DOX-loaded st-PLGA–PEG micelles with different arm numbers, the concentration at which 50 % of cells were killed in a given period (48 h), were obtained from the cell viability data and are shown in Fig. 10e. It appears that 4s-PLGA–PEG micelles had the most potent activity among the three star-shaped copolymers (3s/4s/6s-PLGA–PEG). As aforementioned analysis, arm numbers of st-PLGA–PEG block copolymers had an important influence on internalization of the micelles and DOX release properties from the micelles. The characteristics of 4s-PLGA–PEG micelles, including the micelles' size, surface PEG distribution and drug release behavior, facilitated their cellular uptake and a higher release efficiency of DOX after internalization within cells. Thus it can be seen that the IC50 values of 4s-PLGA–PEG micelles (2.75 μg/mL) was less than half of those of 3s-PLGA–PEG micelles (5.26 μg/mL) and 6s-PLGA–PEG micelles (3.43 μg/mL).

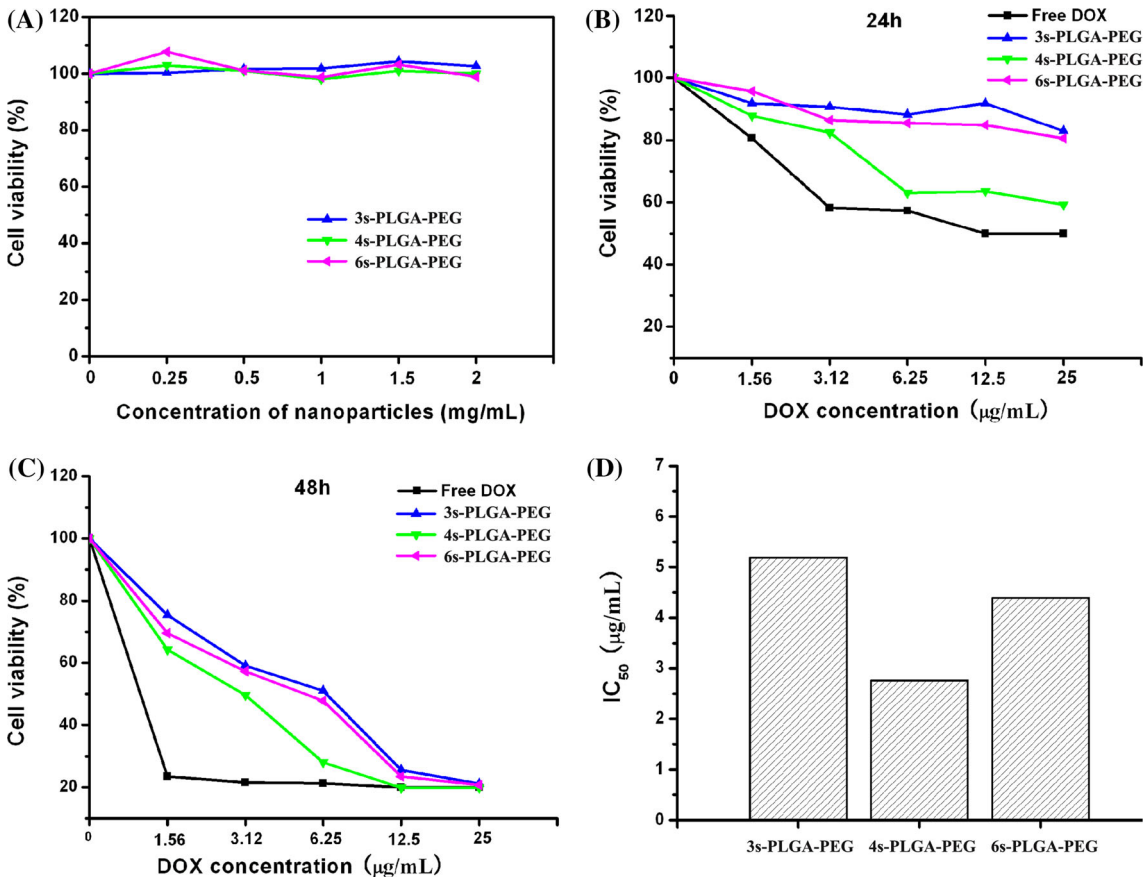

Fig. 10 In vitro cytotoxicity of empty st-PLGA–PEG micelles with different arm numbers after 48 h incubation with HeLa cells (**a**). In vitro cytotoxicity of free DOX and DOX-loaded st-PLGA–PEG micelles with different arm numbers after 24 h (**b**) and 48 h (**c**) incubation with HeLa cells. IC_{50} values of DOX-loaded st-PLGA–PEG micelles after 48 h incubation with HeLa cells (D) (n = 5). Compared with 3s-PLGA–PEG micelles and 6s-PLGA–PEG micelles, a significant reduction in IC_{50} values for 4s-PLGA–PEG micelles could be observed ($P < 0.05$)

4 Conclusion

Well-defined st-PLGA–PEG copolymers with different arm numbers (3s/4s/6s-PLGA–PEG) were successfully synthesized to investigate the relationship between the arm numbers of st-PLGA–PEG copolymers and their micelle properties. The CMC value of st-PLGA–PEG copolymers decreased with increasing the arms in st-PLGA–PEG copolymers, indicating that the micelle formation becomes easier as the number of arm in st-PLGA–PEG copolymers increases. The model drug DOX was effectively loaded in the polymeric micelles. The size of DOX-loaded micelles and drug loading content also increased in the same order as in the case of the CMC. DOX-loaded micelles with different arm numbers in st-PLGA–PEG copolymers could achieve a controlled release behavior. The effects of arm numbers in st-PLGA–PEG copolymers on cellular uptake and cytotoxicity of DOX-loaded micelles in vitro were systematically investigated in HeLa cells. The DOX-loaded 4s-PLGA–PEG micelles possess the highest efficiency of cellular uptake and cytotoxicity among the three star-shaped copolymers (3s/4s/6s-PLGA–PEG), probably because of the difference in micelles size and PEG distribution on the surface of st-PLGA–PEG micelles. Thus structural tailoring of arm numbers from st-PLGA–PEG copolymers could provide a new strategy for designing drug carriers of high efficiency.

Acknowledgments The authors are grateful to the Natural Science Foundation of China (Nos. 50903093 and 51373199), the Tianjin Natural Science Foundation project (Nos. 15JCYBJC18400 and 15JCZDJC38300), PUMC Youth Fund and the Fundamental Research Funds for the Central Universities (No. 33320140188).

References

1. Letchford K, Burt H. A review of the formation and classification of amphiphilic block copolymer nanoparticulate structures: micelles, nanospheres, nanocapsules and polymersomes. Eur J Pharm Biopharm. 2007;65:259–69.

2. Xiong XB, Falamarzian A, Garg SM, Lavasanifar A. Engineering of amphiphilic block copolymers for polymeric micellar drug and gene delivery. J Control Release. 2011;155:248–61.
3. Ren WH, Chang J, Yan CH, Qian XM, Long LX, He B, Yuan XB, Kang CS, Betbeder D, Sheng J, Pu PY. Development of transferrin functionalized poly(ethylene glycol)/poly(lactic acid) amphiphilic block copolymeric micelles as a potential delivery system targeting brain glioma. J Mater Sci Mater Med. 2010;21:2673–81.
4. Cai TT, Lei Q, Yang B, Jia HZ, Cheng H, Liu LN, Zeng X, Feng J, Zhuo RX, Zhang XZ. Utilization of H-bond interaction of nucleobase uralic with antitumor methotrexate to design drug carrier with ultrahigh loading efficiency and pH-responsive drug release. Regen Biomater. 2014;1:27–36.
5. Torchilin VP. Micellar nanocarriers: pharmaceutical perspectives. Pharm Res. 2007;24:1–16.
6. Croy SR, Kwon GS. Polymeric micelles for drug delivery. Curr Pharm Des. 2006;12:4669–84.
7. Mahmud A, Xiong XB, Aliabadi HM, Lavasanifar A. Polymeric micelles for drug targeting. J Drug Target. 2007;15:553–84.
8. Kwon GS, Kataoka K. Block copolymer micelles as long circulating drug vehicles. Adv Drug Deliv Rev. 1995;16:295–309.
9. Huang X, Xiao Y, Lang M. Self-assembly of pH-sensitive mixed micelles based on linear and star copolymers for drug delivery. J Colloid Interface Sci. 2011;364:92–9.
10. Namazi H, Jafarirad S. In vitro photo-controlled drug release system based on amphiphilic linear-dendritic diblock copolymers; self-assembly behavior and application as nanocarrier. J Pharm Pharmaceut Sci. 2011;14:162–80.
11. Liu XM, Pramoda KP, Yang YY, Chow SY, He C. Cholesteryl-grafted functional amphiphilic poly(*N*-isopropylacrylamide-*co*-*N*-hydroxylmethylacrylamide): synthesis, temperature-sensitivity, self-assembly and encapsulation of a hydrophobic agent. Biomaterials. 2004;25:2619–28.
12. Ambade AV, Savariar EN, Thayumanavan S. Dendrimeric micelles for controlled drug release and targeted delivery. Mol Pharm. 2005;2:264–72.
13. Li X, Qian Y, Liu T, Hu X, Zhang G, You Y, Liu S. Amphiphilic multiarm star block copolymer-based multifunctional unimolecular micelles for cancer targeted drug delivery and MR imaging. Biomaterials. 2011;32:6595–605.
14. Jie P, Venkatraman SS, Min F, Freddy BY, Huat GL. Micelle-like nanoparticles of star-branched PEO–PLA copolymers as chemotherapeutic carrier. J Control Release. 2005;110:20–33.
15. Peng CL, Shieh MJ, Tsai MH, Chang CC, Lai PS. Self-assembled star-shaped chlorin-core poly(epsilon-caprolactone)-poly(ethylene glycol) diblock copolymer micelles for dual chemo-photodynamic therapies. Biomaterials. 2008;29:3599–608.
16. Heise A, Hedrick JL, Frank CW, Miller RD. Star like block copolymers with amphiphilic arms as models for unimolecular micelles. J Am Chem Soc. 1999;121:8647–8.
17. Quaglia F, Ostacolo L, De Rosa G, La Rotonda MI, Ammendola M, Nese G, Maglio G, Palumbo R, Vauthier C. Nanoscopic core-shell drug carriers made of amphiphilic triblock and star-diblock copolymers. Int J Pharm. 2006;324:56–66.
18. Lele BS, Leroux JC. Synthesis of novel amphiphilic star-shaped poly(ε-caprolactone)-block-poly(*N*-(2-hydroxypropyl)methacrylamide) by combination of ring-opening and chain transfer polymerization. Polymer. 2002;43:5595–606.
19. Poree DE, Giles MD, Lawson LB, He J, Grayson SM. Synthesis of amphiphilic star block copolymers and their evaluation as transdermal carriers. Biomacromolecules. 2011;12:898–906.
20. Zhu J, Zhou Z, Yang C, Kong DL, Wan Y, Wang Z. Folate-conjugated amphiphilic star-shaped block copolymers as targeted nanocarriers. J Biomed Mater Res A. 2011;97:498–508.
21. Quaglia F, Ostacolo L, Nese G, Canciello M, De Rosa G, Ungaro F, Palumbo R, La Rotonda MI, Maglio G. Micelles based on amphiphilic PCL–PEO triblock and star-shaped diblock copolymers: potential in drug delivery applications. J Biomed Mater Res A. 2008;87:563–74.
22. Hua C, Dong CM. Synthesis, characterization, effect of architecture on crystallization of biodegradable poly(epsilon-caprolactone)-*b*-poly(ethylene oxide) copolymers with different arms and nanoparticles thereof. J Biomed Mater Res A. 2007;82:689–700.
23. Kim KH, Cui GH, Lim HJ, Huh J, Ahn CH, Jo WH. Synthesis and micellization of star-shaped poly(ethylene glycol)-block-poly(ε-caprolcatone). Macromol Chem Phys. 2004;205:1684–92.
24. Qiu LY, Bae YH. Polymer architecture and drug delivery. Pharm Res. 2006;23:1–30.
25. Malmo J, Varum KM, Strand SP. Effect of chitosan chain architecture on gene delivery: comparison of self-branched and linear chitosans. Biomacromolecules. 2011;12:721–9.
26. Ooya T, Lee J, Park K. Effects of ethyleneglycol-based graft, star-shaped, and dendritic polymers on solubilization and controlled release of paclitaxel. J Control Release. 2006;93:121–7.
27. Yoon JJ, Chung HJ, Lee HJ, Park TG. Heparin-immobilized biodegradable scaffolds for local and sustained release of angiogenic growth factor. J Biomed Mater Res A. 2008;79:934–42.
28. Wang DD, Peng ZhP, Liu XX, Tong Zh, Wang ChY, Ren BY. Synthesis and micelle formation of triblock copolymers of poly(methyl methacrylate)-*b*-poly(ethylene oxide)-*b*-poly(methyl methacrylate) in aqueous solution. Euro Polym J. 2007;43:2799–808.
29. Ge HX, Hu Y, Jiang XQ, Cheng DM, Yuan YY, Bi H, Yang CZ. Preparation, characterization, and drug release behaviors of drug nimodipine-loaded poly (ε-caprolactone)-poly(ethylene oxide)-poly (ε-caprolactone) amphiphilic triblock copolymer micelles. J Pharm Sci. 2002;91:1463–73.
30. Yan F, Zhang C, Zheng Y, Mei L, Tang LN, Song CX, Sun HF, Huang LQ. The effect of poloxamer 188 on nanoparticle morphology, size, cancer cell uptake, and cytotoxicity. Nanomedicine. 2010;6:170–8.
31. Podzimek S. The use of GPC coupled with a multiangle laser light scattering photometer for the characterization of polymers. On the determination of molecular weight, size, and branching. J Appl Polym Sci. 1994;54:91–103.
32. Claesson H, Malmstrom E, Johansson M, Hult A. Synthesis and characterization of star branched polyesters with dendritic cores and the effect of structural variations on zero shear rate viscosity. Polymer. 2002;43:3511–8.
33. Oda K, Matsuoka Y, Funahashi A, Kitano H. A comprehensive pathway map of epidermal growth factor receptor signaling. Mol Syst Biol. 2005;1:11–7.
34. Perrault SD, Walkey C, Jennings T, Fischer HC, Chan WC. Mediating tumor targeting efficiency of nanoparticles through design. Nano Lett. 2009;9:1909–15.
35. Yuan F, Dellian M, Fukumura D, Leunig M, Berk DA, Torchilin VP, Jain RK. Vascular permeability in a human tumor xenograft: molecular size dependence and cutoff size. Cancer Res. 1995;55:3752–6.
36. Liu XN, Li XR, Zhou L, Li SB, Sun J, Wang ZL, Gao Y, Jiang Y, Lu HB, Wang QB, Dai JW. Effects of simvastatin-loaded polymeric micelles on human osteoblast-like MG-63 cells. Colloids Surf B Biointerfaces. 2014;10:420–7.
37. Yang YQ, Zhao B, Li ZD, Lin WJ, Zhang CY, Guo XD, Wang JF, Zang LJ. pH-sensitive micelles self-assembled from multi-arm star triblock co-polymers poly(ε-caprolactone)-*b*-poly(2-(diethylamino)ethyl methacrylate)-*b*-poly(poly(ethylene glycol) methyl ether methacrylate) for controlled anticancer drug delivery. Acta Biomater. 2013;9:7679–90.
38. Pamujula S, Hazari S, Bolden G, Graves RA, Chinta DD, Dash S, Kishore V, Mandal TK. Cellular delivery of PEGylated PLGA nanoparticles. J Pharm Pharmacol. 2012;64:61–7.

39. Xiao K, Li Y, Luo J, Lee JS, Xiao W, Gonik AM, Agarwal RG, Lam KS. The effect of surface charge on in vivo biodistribution of PEG-oligocholic acid based micellar nanoparticles. Biomaterials. 2011;32:3435–46.
40. Zhang C, Wang W, Liu T, Wu Y, Guo H, Wang P, Tian Q, Wang YM, Yuan Z. Doxorubicin-loaded glycyrrhetinic acid-modified alginate nanoparticles for liver tumor chemotherapy. Biomaterials. 2012;33:2187–96.
41. Holgado MA, Arias JL, Cozar MJ, Alvarez-Fuentes J, Ganan-Calvo AM, Fernandez-Arevalo M. Synthesis of lidocaine-loaded PLGA microparticles by flow focusing: effects on drug loading and release properties. Int J Pharm. 2008;358:27–35.
42. Yoo HS, Park TG. Biodegradable polymeric micelles composed of doxorubicin conjugated PLGA–PEG block copolymer. J. Control Release. 2011;70:63–70.
43. Gillies ER, Frechet JMJ. pH-responsive copolymer assemblies for controlled release of doxorubicin. Bioconjugate Chem. 2005;16:361–8.
44. Chittasupho C, Xie SX, Baoum A, Yakovleva T, Siahaan TJ, Berkland CJ. ICAM-1 targeting of doxorubicin-loaded PLGA nanoparticles to lung epithelial cells. Eur J Pharm Sci. 2009; 37:141–50.
45. Gustafson DL, Merz AL, Long ME. Pharmacokinetics of combined doxorubicin and paclitaxel in mice. Cancer Lett. 2005; 220:161–9.
46. Sieczkowski E, Lehner C, Ambros PF, Hohenegger M. Double impact on p-glycoprotein by statins enhances doxorubicin cytotoxicity in human neuroblastoma cells. Int J Cancer. 2010;126:2025–35.
47. Xu A, Yao M, Xu G, Ying J, Ma W, Li B, Jin Y. A physical model for the size-dependent cellular uptake of nanoparticles modified with cationic surfactants. Int J Nanomed. 2012;7:3547–54.
48. Wang SH, Lee CW, Chiou A, Wei PK. Size-dependent endocytosis of gold nanoparticles studied by three-dimensional mapping of plasmonic scattering images. J Nanobiotechnol. 2012;8:33.
49. Hak S, Helgesen E, Hektoen HH, Huuse EM, Jarzyna PA, Mulder WJM, Haraldseth O, De Lange Davies C. The effect of nanoparticle polyethylene glycol surface density on ligand-directed tumor targeting studied in vivo by dual modality imaging. ACS Nano. 2012;6:5648–58.
50. Sun H, Guo B, Li X, Cheng R, Meng F, Liu H, Zhong Z. Shell-sheddable micelles based on dextran-SS-poly(ε-caprolactone) diblock copolymer for efficient intracellular release of doxorubicin. Biomacromolecules. 2010;11:848–54.
51. Liu SQ, Wiradharma N, Tong YW, Gao SJ, Yang YY. Bio-functional micelles self-assembled from a folate-conjugated block copolymer for targeted intracellular delivery of anticancer drugs. Biomaterials. 2007;28:1423–33.
52. Zhao H, Yung LYL. Selectivity of folate conjugated polymer micelles against different tumor cells. Int J Pharm. 2008;349:256–68.
53. Minotti G, Menna P, Salvatorelli E, Cairo G, Gianni L. Anthracyclines: molecular advances and pharmacologic developments in antitumor activity and cardiotoxicity. Pharmacol Rev. 2004;56:185–229.